

- Seinfeld, *Environ. Sci. Technol.* **21**, 1224 (1987); M. W. Gery, D. L. Fox, H. E. Jeffries, *Int. J. Chem. Kinet.* **17**, 931 (1985); J. A. Leone, R. C. Flagan, D. Grosjean, J. H. Seinfeld, *ibid.*, p. 177; D. Grosjean, in *Ozone and Other Photochemical Oxidants* (National Academy of Sciences, Washington, DC, 1977), chap. 3.
9. R. A. Harley, M. P. Hannigan, G. R. Cass, *Atmos. Environ. A* **26**, 2395 (1992).
 10. J. R. Odum *et al.*, *Environ. Sci. Technol.* **30**, 2580 (1996).
 11. Initial hydrocarbon concentrations ranged from 400 to 5000 $\mu\text{g m}^{-3}$ for the individual aromatic experiments and from 2700 to 7000 $\mu\text{g m}^{-3}$ for the gas-line experiments. Concentrations of NO_x ($\text{NO} + \text{NO}_2$) were selected so that HC/NO_x ratios typical of those in an urban environment (5 to 10 ppbC/ppb NO_2) were achieved. The ratio of NO/NO_2 was always set at 2.
 12. Scanning electrical mobility spectrometers were used to obtain complete particle number and size distributions with a 1-min frequency. Time-dependent particle volume concentrations were calculated from these distributions. The time-dependent cumulative organic volume concentration was calculated by subtracting the volume concentration at time t (corrected for deposition) from the initial volume concentration. Total organic mass concentrations were calculated from the total cumulative organic volume concentration assuming the density of the condensed organic phase was 1 g cm^{-3} .
 13. J. F. Pankow, *Atmos. Environ. A* **28**, 185 (1994).
 14. Parameter K_{om} is an equilibrium constant describing the partitioning of semivolatile organics between the vapor phase and an absorbing organic condensed phase: $K_{\text{om}} = (F/M_o)/A$, where F and A are a semivolatile compound's concentration in the absorbing organic and vapor phases, respectively, and M_o is the concentration of the absorbing organic aerosol.
 15. AQIRP was a cooperative program whose members included three domestic auto companies and 14 petroleum companies, the objective of which was to develop data on the potential improvements in vehicle emissions and air quality, primarily O_3 , from reformulated gasoline, various other alternative fuels, and developments in automotive technology. V. R. Burns *et al.*, *SAE Tech. Pap. 912320* (Society of Automotive Engineers, Warren, PA, 1991); A. M. Hochhauser *et al.*, *SAE Tech. Pap. 912322* (Society of Automotive Engineers, Warren, PA, 1991).
 16. R. H. Paul and M. J. McNally, *SAE Tech. Pap. 902098* (Society of Automotive Engineers, Warren, PA, 1991); W. O. Siegl *et al.*, *SAE Tech. Pap. 930142* (Society of Automotive Engineers, Warren, PA, 1993).
 17. Hydroxyl radical and O_3 rate constants were taken from review literature (20) and the National Institute of Standards and Technology (NIST) chemical kinetics database (21) or, when experimentally not known, were estimated with the structure reactivity relations (SARs) (22). The SAR expressions for alkanes and alkenes were used unchanged; we modified those for aromatics by deriving a new Hammett constant for metasubstituents (σ_m^+). We optimized σ_m^+ for the ring addition rate constant (k_{add}) of 15 alkyl-substituted aromatics. The expression derived for use within SAR was $\log_{10} k_{\text{add}} (\text{cm}^3 \text{ molecule}^{-1} \text{ s}^{-1}) = -11.89 - 1.82 \sum \sigma_m^+$, where $\sigma^+ = \sigma_m^+$ and $\sigma_{\text{ortho,p}}^+$ with $\sigma_m^+ = -0.190$ for all meta-alkyl substituents and Hammett constants for ortho and para substituents ($\sigma_{\text{ortho,p}}^+$) as used in (22). The quality of the fit for the overall OH rate constant estimates for aromatics was improved to 30% maximum error, compared to 110% using the parameters in (22).
 18. The value of Δ_{aromatic} was calculated by summing the reacted amount of each aromatic species in a fuel for a given experiment. The ratio of $\Delta M_o/\Delta_{\text{aromatic}}$ is a measure of the SOA yield of a fuel in terms of its aromatic fraction only. For the individual aromatic experiments, $\Delta M_o/\Delta_{\text{aromatic}} = Y$.
 19. For most fuels, 92 to 99% of the mass was speciated in AQIRP (16). Only 83% of the mass of fuel RF-L, which was the only high T_{90} AQIRP Phase I fuel used in this study, was speciated in AQIRP (23). Much of the remaining 17% of the mass of this fuel is most likely heavy aromatic species that contribute to the

SOA formed from the oxidation of this fuel. Because this 17% was not speciated, Δ_{aromatic} for this fuel is most likely underestimated, explaining why this fuel does not fall within the envelope as all other fuels specified by curves 1 and 2 (Fig. 2).

20. R. Atkinson, *J. Phys. Chem. Ref. Data Monogr.* **2** (1994).
21. NIST Chemical Kinetics Database ver. 6.01; W. G. Mallard, F. Westley, J. T. Herron, R. F. Hampson, NIST Standard Reference Data, Gaithersburg, MD (1994).
22. E. S. C. Kwok and R. Atkinson, *Atmos. Environ. A* **29**, 1685 (1995).
23. Temperature T_{90} is the distillation temperature at which 90% of the fuel evaporates. It relates to a fuel's heavy-end volatility: Fuels with high T_{90} contain a significant fraction of heavy components. In

Phase I of the AQIRP, only 143 compounds were speciated, and many of the heavy components (including aromatics) were not accounted for. In Phase II, 320 compounds were speciated, and many of the heavier aromatics were accounted for. Thus, more than 94% of the carbon, on average, was accounted for in all Phase II fuels (both high and low T_{90}).

24. We would like to acknowledge support by the U.S. Environmental Protection Agency Center on Airborne Organics, the National Science Foundation, the Deutsche Forschungsgemeinschaft, the Coordinating Research Council, and the Chevron Corporation. We would also like to thank S. Kent Hoekman for his helpful comments.

2 December 1996; accepted 5 February 1997

Metathesis of Alkanes Catalyzed by Silica-Supported Transition Metal Hydrides

Véronique Vidal, Albert Théolier, Jean Thivolle-Cazat, Jean-Marie Basset*

The silica-supported transition metal hydrides ($\equiv\text{Si-O-Si}\equiv$)($\equiv\text{Si-O}$)₂Ta-H and ($\equiv\text{Si-O}$)_xM-H (M, chromium or tungsten) catalyze the metathesis reaction of linear or branched alkanes into the next higher and lower alkanes at moderate temperature (25° to 200°C). With ($\equiv\text{Si-O-Si}\equiv$)($\equiv\text{Si-O}$)₂Ta-H, ethane was transformed at room temperature into an equimolar mixture of propane and methane. Higher and lower homologs were obtained from propane, butane, and pentane as well as from branched alkanes such as isobutane and isopentane. The mechanism of the step leading to carbon-carbon bond cleavage and formation likely involves a four-centered transition state between a tantalum-alkyl intermediate and a carbon-carbon σ -bond of a second molecule of alkane.

Paraffins, particularly methane and light alkanes, constitute an abundant yet low-value fossil feedstock. Light alkanes would be very valuable if they could be transformed into higher molecular weight hydrocarbons (1); this represents a continuing scientific challenge (2). Here, we report observations of a catalytic reaction that we designate "metathesis of alkanes" and which, to our knowledge, has not previously been reported (3). The metathesis reaction proceeds by both the cleavage and the formation of the C-C bonds of acyclic alkanes, which are transformed into a mixture of higher and lower homologs. It was observed in the presence of various silica-supported metal-hydride catalysts, particularly tantalum hydride (4), all prepared by the surface organometallic chemistry route (5, 6). Metathesis reactions of alkenes and alkynes, discovered a few decades ago, are now well documented and understood and are used in several industrial chemical processes. In contrast to the metathesis of alkenes (7) or alkynes (8), for which the cleavage of the molecule occurs selectively at the C=C or

C \equiv C bond, the metathesis of acyclic alkanes seems to involve, at least to some extent, the reaction of all C-C bonds. Thus, the reaction, even if it is selective in terms of the formation and cleavage of C-C bonds, is not restricted to the formation of the first higher and lower homologs but also can yield the next several higher and lower ones. The metathesis of acyclic olefins is hindered by thermodynamic limitations; such a reaction is close to thermoneutrality for most alkanes (9).

We recently reported that the reaction of Ta(-CH₂CMe₃)₃(=CHCMe₃) (Me, methyl) (10) with the surface hydroxyl groups of a dehydroxylated silica (11) leads to the formation of a mixture of two species: ($\equiv\text{Si-O}$)Ta(-CH₂CMe₃)₂(=CHCMe₃) (~65%) and ($\equiv\text{Si-O}$)₂Ta(-CH₂CMe₃) (=CHCMe₃) (~35%) (12). Treatment of these two surface complexes under hydrogen at 150°C overnight yields mainly a surface tantalum (III) monohydride, ($\equiv\text{Si-O-Si}\equiv$)($\equiv\text{Si-O}$)₂Ta-H ([Ta]_s-H), which has been fully characterized by infrared spectroscopy, extended x-ray absorption fine structure (EXAFS) analysis, microanalysis, and quantitative chemical reactions (4).

When [Ta]_s-H was contacted at room temperature with a cyclic alkane (4, 13), no catalytic reaction occurred. Only a C-H

Laboratoire de Chimie Organométallique de Surface, UMR CNRS-CPE 9986, 43 Boulevard du 11 Novembre 1918, 69616 Villeurbanne Cédex, France.

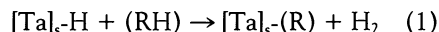
*To whom correspondence should be addressed.

Table 1. Metathesis reaction of acyclic alkanes catalyzed by the [Ta]₅-H complex at 150°C.

Alkanes*	TON†	Selectivity of alkanes produced (%)											
		Meth- ane	Eth- ane	Pro- pane	Bu- tane	Iso- butane	<i>n</i> -Pen- tane	Iso- pentane	Neo- pentane	<i>n</i> -Hex- ane	Iso- hexane	Hep- tanes‡	Oc- tanes‡
Ethane	46	53	–	44	2.4	0.6							
Ethane§	3	37		63									
Propane	47	15.7	37.4	–	27.2	6.7	6.5	3.2		2.2	1.2		
Propane	12	1.9	59	–	31	2	4.8	0.6		0.7			
Butane	66	2	12.5	36	–	3.5	26.5	3	0	10	1	4.5	1
Isobutane	17	12	22	20.5	0.6	–	0	18.6	5.2	0	13	7	4
Pentane	12	0.8	4	16.5	32	0.5	–	–	–	24.5	3	12.7	6

*Gaseous alkanes: 1 atm, alkane/Ta ratio ≈ 800; pentane: 400 torr, C₅/Ta ratio ≈ 400; reaction time: 50 to 80 hours. †The turnover number (TON) is the average number of alkane molecules transformed per mole of Ta during the experiment. ‡Linear and branched alkanes. §Catalyzed by silica-supported chromium hydride. ||Catalyzed by silica-supported tungsten hydride.

bond activation was observed, which led to the stoichiometric formation of a tantalum (III)-cycloalkyl species with the evolution of 1 mol of hydrogen. Tantalum is extremely electrophilic, and thus we assume that this activation occurs by a σ -bond metathesis



(where R = cyclopentyl, cyclohexyl, cycloheptyl, or cyclooctyl), rather than by an oxidative addition-reductive elimination pathway (13). When [Ta]₅-H was contacted with an acyclic alkane, a catalytic metathesis reaction occurred at moderate temperature (25° to 200°C), leading to the formation of the higher and lower homologs (Table 1). The simplest case is the metathesis of ethane, which has only one C–C bond and consequently does not present any problem of selectivity. This alkane yielded propane and methane in comparable amounts, as well as trace amounts of *n*-butane and isobutane (Fig. 1). In this example, it is clear that a methyl fragment is transferred from one molecule of ethane to a second one. A labeling experiment carried out with ¹³C-monolabeled ethane yielded unlabeled, monolabeled, dilabeled, and trilabeled propane (5:44:43:8), which proved the cleavage of the ¹³C–¹²C bond of ethane and the redis-

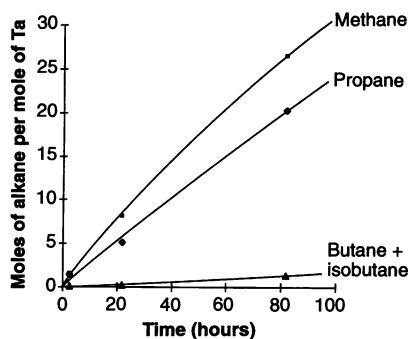


Fig. 1. Metathesis reaction of ethane catalyzed by the silica-supported [Ta]₅-H complex at 150°C under 1 atm (C₂H₆/Ta ratio, ~800).

tribution of the ¹³C atoms into the propane molecules.

When higher linear alkanes were used, several higher and lower homologs were produced, because various C–H and C–C bonds can be involved. For example, metathesis of propane yielded mainly *n*-butane and isobutane together with ethane, and *n*-butane yielded *n*-pentane and isopentane as well as propane; besides these main products, some higher and lower alkanes were also produced (Fig. 2). This suggests, as observed for ethane, that the main reaction involves the transfer of a methyl fragment from one molecule of the initial alkane to a second one; the wider product distribution observed with higher alkanes (for example, butane and pentane) (Fig. 2) also suggests the probable occurrence of secondary reactions, the possible transfer of higher alkyl fragments such as ethyl, or both. The occurrence of the two processes can hardly be distinguished; secondary reactions can take place as the reaction proceeds and the conversion increases. (The two related processes

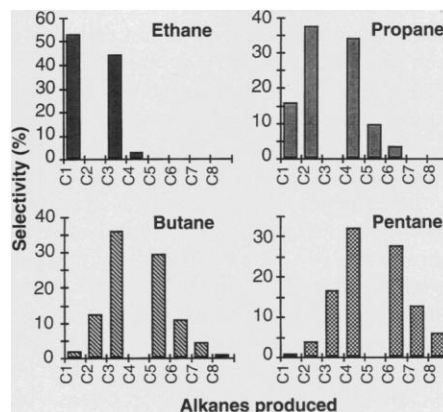
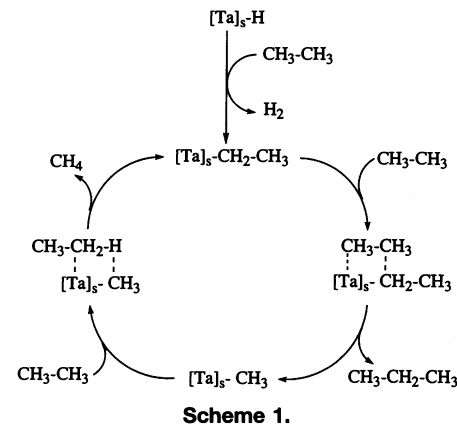


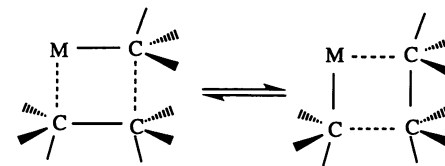
Fig. 2. Distribution of the various hydrocarbons produced during the metathesis reaction of the first lower linear alkanes (at 3% conversion), catalyzed by the silica-supported [Ta]₅-H complex at 150°C (ethane, propane, or butane/Ta ratio, ~800, *P* = 1 atm; pentane/Ta ratio, ~400, *P* = 400 torr). The starting alkane in excess is not represented.

may possibly be distinguished by a kinetic study in a dynamic reactor with varying contact time.) All the alkanes present in the medium can be presumed to compete for the adsorption. In the case of ethane, secondary reactions seem to occur very soon with the appearance of butane and especially isobutane, the formation of which necessarily arises from a secondary reaction of propane. Branched alkanes such as isobutane or methyl butane also underwent the metathesis reaction; however, neopentane only led to the stoichiometric formation of a surface tantalum-neopentyl species and did not react further, probably for steric reasons.

During the metathesis reaction, infrared spectroscopy showed that the tantalum hydride disappeared and was transformed into a tantalum-alkyl intermediate. At 150°C, aging of the catalyst was observed, preventing higher conversions. In a few exploratory experiments, it was observed that similar

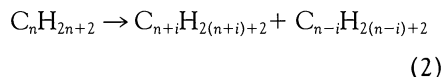


Scheme 1.

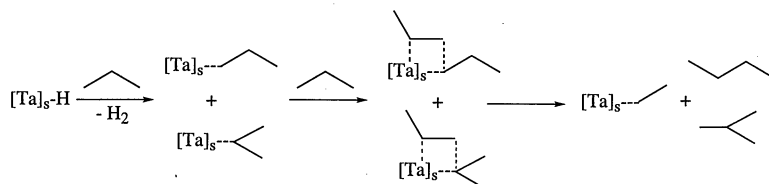


Scheme 2.

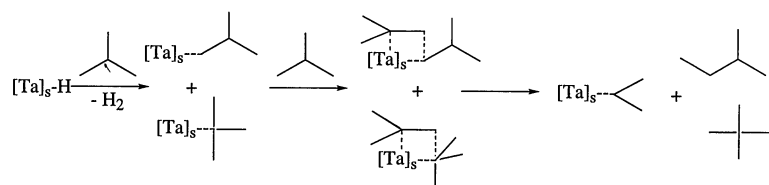
silica-supported hydrides of tungsten or chromium (14) were also able to catalyze the alkane metathesis reaction (Table 1), whereas silica-supported hydrides of zirconium, hafnium, or aluminum (14) did not show any activity. To our knowledge, this alkane metathesis reaction is an unprecedented catalytic reaction; it can be described by the general equation



with $i = 1, 2, \dots, n-1$, but where $i = 1$ is generally favored.



Scheme 3.



Scheme 4.

Regarding the mechanism of the reaction (15) (Scheme 1), we assume that in a first step, a C-H bond of acyclic alkane (for example, ethane) is cleaved by a σ -bond metathesis, producing hydrogen and a tantalum-alkyl (for example, ethyl) species; this elementary step is indeed observed during the C-H bond activation of cycloalkanes on the $[Ta]_s-H$ species, yielding the corresponding tantalum-cycloalkyl surface complexes (Eq. 1), and occurs without modification of the oxidation state of the metal (4). The next step involves the transfer of a methyl group and necessarily implies the cleavage and the formation of C-C bonds. Among the known elementary steps, two possibilities can be considered: (i) The oxidative addition of the ethane C-C bond (16) would yield the dimethyl(ethyl)tantalum(V) surface complex; reductive elimination of propane from this complex could follow, with the concomitant release of a tantalum-methyl species. (ii) A σ -bond metathesis mechanism, which we prefer because of the highly electrophilic character of the silica-supported tantalum-alkyl species, would involve a four-centered transition state with the presence of an sp^3 carbon in the middle of the metallocycle (Scheme 2).

Related but different four-centered intermediates, in which a hydrogen atom replaces the central carbon, have been invoked in recent studies concerning the

C-H bond activation of alkanes (17); other four-centered intermediates have been proposed in the dehydropolymerization of silane compounds (18). In the case of ethane, this step of C-C bond formation and cleavage enables the liberation of propane and the formation of a tantalum-methyl surface complex. The last step in the catalytic cycle must liberate methane and regenerate the active species, the tantalum-ethyl surface complex; a new four-centered transition state is assumed in which a hydrogen is transferred from an ethane molecule to the methyl ligand (Scheme 1).

Such a mechanism is also operating in the case of higher alkanes. For example, the formation of *n*-butane and isobutane from propane is determined in the first step of C-H bond activation, which yields two species, tantalum-*n*-propyl and tantalum-isopropyl surface complexes (Scheme 3). The subsequent transfer of a methyl group from a second propane molecule to these propyl intermediates enables the evolution of *n*-butane and isobutane as well as the formation of a tantalum-ethyl complex, which in turn will yield ethane.

The metathesis of isobutane is particularly interesting with respect to the product distribution. In agreement with the proposed mechanism, the C-H bond activation step can produce two tantalum-alkyl intermediates (Scheme 4). We can expect that the formation of the tantalum-*tert*-butyl species can be disfavored (relative to that of the other possible tantalum-isobutyl complex) for steric reasons; despite this, the production of neopentane resulting from the methyl transfer step on the tantalum-*tert*-butyl occurs in substantial amounts.

REFERENCES AND NOTES

1. H. Mimoun, *New J. Chem.* **11**, 513 (1987).
2. M. M. Bhasin and D. W. Slocum, Eds., *Methane and Alkane Conversion Chemistry* (Plenum, New York, 1995).

3. CNRS, French Patent No. 96 09033.
4. V. Vidal, A. Théolier, J. Thivolle-Cazat, J. M. Basset, J. Coker, *J. Am. Chem. Soc.* **118**, 4595 (1996).
5. Y. Iwasawa, Ed., *Tailored Metal Catalysts* (Reidel, Dordrecht, Netherlands, 1986).
6. F. Quignard, A. Choplin, J. M. Basset, *J. Chem. Soc. Chem. Commun.* **1991**, 1589 (1991); F. Quignard, C. Lécuyer, A. Choplin, D. Olivier, J. M. Basset, *J. Mol. Catal.* **74**, 353 (1992); C. Lécuyer, F. Quignard, A. Choplin, D. Olivier, J. M. Basset, *Angew. Chem. Int. Ed. Engl.* **30**, 1660 (1991); F. Quignard, C. Lécuyer, A. Choplin, J. M. Basset, *J. Chem. Soc. Dalton Trans.* **1994**, 1153 (1994); F. Quignard *et al.*, *Inorg. Chem.* **31**, 928 (1992); J. Coker *et al.*, *Science* **271**, 966 (1996).
7. R. L. Banks and G. C. Bailey, *Ind. Eng. Chem. Prod. Res. Dev.* **3**, 170 (1964); G. Natta, C. D. Dall'Asta, G. Mazzanti, *Angew. Chem. Int. Ed. Engl.* **3**, 723 (1964); N. Calderon, *Acc. Chem. Res.* **5**, 127 (1972); H. S. Eleuterio, *J. Mol. Catal.* **65**, 55 (1991); K. J. Ivin, *Olefin Metathesis* (Academic Press, London, 1983).
8. A. Mortreux, F. Petit, M. Blanchard, *Tetrahedron Lett.* **49**, 4967 (1978).
9. The reaction enthalpy for the metathesis of ethane to propane and methane ($2C_2H_6 \rightleftharpoons C_3H_8 + CH_4$) at 400 K is $\Delta H^0 = -2.15$ kcal mol⁻¹, whereas the standard free energy variation is $\Delta G^0 = -1.98$ kcal mol⁻¹. These values were calculated from data found in D. R. Stull, E. F. Westrum Jr., G. C. Sinke, *The Chemical Thermodynamics of Organic Compounds* (Krieger, Malabar, FL, 1987).
10. R. R. Schrock and J. D. Fellmann, *J. Am. Chem. Soc.* **100**, 3359 (1978).
11. Aerosil Degussa silica (200 m²/g) was dehydroxylated at 500°C under vacuum [(SiO₂)₅₀₀].
12. V. Dufaud, G. P. Niccolai, J. Thivolle-Cazat, J. M. Basset, *J. Am. Chem. Soc.* **117**, 4288 (1995).
13. V. Vidal, A. Théolier, J. Thivolle-Cazat, J. M. Basset, *J. Chem. Soc. Chem. Commun.* **1995**, 991 (1995).
14. To obtain silica-supported tungsten hydride, we allowed tris(neopentyl)neopentylidyne tungsten, W(CH₂-CMe₃)₃(=C-CMe₃) [R. R. Schrock, *Inorg. Synth.* **26**, 4 (1989)], to react with the silanols of (SiO₂)₅₀₀. The resulting grafted tungsten complexes were then treated at 80°C under 1 atm of H₂ for 16 hours. Typical bands of W-H were observed at 1942 cm⁻¹. To obtain silica-supported chromium hydride, we allowed Cr(CH₂-SiMe₃)₄ [W. Mowat *et al.*, *J. Chem. Soc. Dalton Trans.* **1972**, 533 (1972)] to react with the OH groups of (SiO₂)₅₀₀. The resulting grafted chromium complex, (=Si-O)Cr(CH₂-SiMe₃)₃ [A. N. Ajiou and S. L. Scott, *Organometallics* **16**, 86 (1997)], was then treated at 150°C under 1 atm of H₂ for 16 hours. Typical bands of Cr-H were observed at 2115 cm⁻¹. To obtain silica-supported zirconium or hafnium hydrides, we allowed Zr(CH₂-CMe₃)₄ or Hf(CH₂-CMe₃)₄ [P. J. Davidson, M. F. Lappert, R. Pearce, *J. Organomet. Chem.* **57**, 269 (1973)] to react with the OH groups of (SiO₂)₅₀₀. The resulting grafted complexes, (=Si-O)Zr(CH₂-CMe₃)₃ and presumably (=Si-O)Hf(CH₂-CMe₃)₃, were then treated at 150°C under 1 atm of H₂ for 16 hours. Typical bands of Zr-H and Hf-H were observed at 1635 and 1702 cm⁻¹, respectively. To obtain silica-supported aluminum hydride, we allowed Al(CH₂-CHMe₂)₃ to react with the OH groups of (SiO₂)₅₀₀. The resulting grafted aluminum complex, presumably (=Si-O)Al(CH₂-CHMe₂)₂, was then treated stepwise at 300°C under 1 atm of H₂. Typical bands of Al-H were observed at 1940 cm⁻¹.
15. In the early stages of the discovery of the olefin metathesis reaction, the most simple mechanism envisaged was a pairwise mechanism in which both olefins would react on the metallic center to give a quasicyclobutane intermediate. This mechanism was later refuted. The simple fact that metathesis of ethane gives methane and propane indicates that the mechanism is nonpairwise, that is, the two alkanes do not play the same role in the mechanism.
16. The oxidative addition of C-C bonds on metallic complexes is a rare process, because it is, in general, thermodynamically disfavored. It has been

mainly observed in the case of strained cycles like cyclopropanes, in the course of stoichiometric reactions [R. A. Periana and R. G. Bergman, *J. Am. Chem. Soc.* **106**, 7272 (1984); R. H. Crabtree, *Chem. Rev.* **85**, 245 (1985); R. J. Puddephatt, *Coord. Chem. Rev.* **33**, 149 (1980)]. It has also been observed with an unstrained C-C bond where the resulting formation of a cyclopentadienyl ligand could be the driving force [R. H. Crabtree and R. P. Dion, *J. Chem. Soc. Chem. Commun.* **1984**, 1260 (1984)]. The oxidative addition of strained cycles

has also been assumed in the course of catalytic processes involving the insertion of olefins [H. Takaya, T. Suzuki, Y. Kumagai, M. Yamakawa, R. Noyori, *J. Org. Chem.* **46**, 2846 (1981); H. Takaya *et al.*, *ibid.*, p. 2854].

17. M. E. Thompson *et al.*, *J. Am. Chem. Soc.* **109**, 203 (1987); P. L. Watson, *ibid.* **105**, 6491 (1983).
18. H. G. Woo, J. F. Walzer, T. D. Tilley, *ibid.* **114**, 7047 (1992).

17 December 1996; accepted 6 February 1997

Thermal Structure of Jupiter's Upper Atmosphere Derived from the Galileo Probe

Alvin Seiff,* Donn B. Kirk, Tony C. D. Knight, Leslie A. Young, Frank S. Milos, Ethiraj Venkatapathy, John D. Mihalov, Robert C. Blanchard, Richard E. Young, Gerald Schubert

Temperatures in Jupiter's atmosphere derived from Galileo Probe deceleration data increase from 109 kelvin at the 175-millibar level to 900 ± 40 kelvin at 1 nanobar, consistent with Voyager remote sensing data. Wavelike oscillations are present at all levels. Vertical wavelengths are 10 to 25 kilometers in the deep isothermal layer, which extends from 12 to 0.003 millibars. Above the 0.003-millibar level, only 90- to 270-kilometer vertical wavelengths survive, suggesting dissipation of wave energy as the probable source of upper atmosphere heating.

The exospheric temperature of Jupiter's upper atmosphere as determined by Voyager solar occultation was 1100 ± 200 K at 1400 km above the 1 bar level (1). This is much hotter than expected based on Jupiter's remoteness from the sun (2). In subsequent fly-by's, Voyager occultations found hot exospheres at the other giant planets (3-5), suggesting that common, non-solar mechanisms were acting to heat giant planet exospheres. Three mechanisms have been proposed: (i) heating by collisions of energetic particles with the neutral upper atmosphere (6), (ii) heating by dissipation of upward propagating gravity waves (7, 8), and (iii) Joule heating by currents in the ionosphere (9). Further progress toward understanding the heating mechanism(s) has

been hampered by the lack of a well-characterized temperature profile (8).

Early analysis of the Galileo probe entry data indicated a jovian exospheric temperature of 1350 K at 800 km altitude, essentially confirming the occultation result (10). Long vertical wavelength oscillations in the temperature profile suggested gravity waves. This analysis assumed that the atmospheric composition did not vary with altitude, the heat shield ablation mass loss was defined by pre-encounter calculations, first-approximation aerodynamics, zero-readings (offsets) of the acceleration sensors on the most sensitive range were unchanged after pre-entry calibration, and a pressure at 1000 km of 2.2 nbar, equivalent to a threshold temperature of 1150 K. Here, we explore the effect of initial pressure, refine the approximations, and revise the profile of Jupiter's middle and upper atmosphere, starting just below the temperature minimum near 175 mb, the tropopause. We also show the development of wavelike oscillations in the temperature structure above the tropopause.

The probe entered the atmosphere at the edge of a 5- μ m hot spot (11) in a near-easterly direction (that is, aligned with planetary rotation) at a relative velocity of 47.4054 km/s along a descending flight path at an angle 8.4104° below horizontal (12). Data acquisition began at 1028 km, where the deduced pressure was ~ 1 nanobar and the molecular mean free path was ~ 0.5 km. This placed the probe deep in the rare gas

or free-molecular flow regime. The transition from free-molecular to continuum flow was between ~ 400 and 300 km altitude. Drag coefficients in rare gas and continuum flow regimes were determined within $\sim 1\%$ by ballistic range tests of scale models and by computational fluid dynamics analysis prior to encounter (13). Probe deceleration was measured over a dynamic range of 10^7 by multi-range accelerometers (14), with uncertainties in sensor scale factor $\sim 0.01\%$ and, in offset (zero reading), ~ 1 count. Data obtained from two independent sensors agreed within ~ 1 count. We have corrected the data for drift in the offset on the most sensitive range based on data taken during a cruise (in-flight) mission simulation test in November 1992. The initial τ_1 offset was increased by 5.7 counts, with 1 count uncertainty. The resulting 17×10^{-6} g correction is important near measurement threshold.

During entry, the probe heat shield was ablated by radiative and convective heating from the shock-layer plasma, which calculations indicate attained a temperature of $\sim 16,000$ K near the 5 mb level (15). Sensors embedded in the heat shield measured the surface recession as a function of time, and were used to calculate changes in probe mass and frontal area as functions of time (16). About one-fourth of the probe mass (90.2 ± 5.8 kg of carbon) was vaporized and/or spalled from the heat shield surface. Variations in probe mass occurred in the late stages of the entry, between 150 km and 80 km altitude, but minor pyrolytic vapor loss occurred after that and was included in the probe mass model. The uncertainty in the mass loss, $\pm 7\%$, left a formal uncertainty of $\pm 2.3\%$ in the residual probe mass, and hence in the atmospheric density below ~ 100 km altitude. At the start of descent, density calculated from pressure and temperature measurements agreed closely with the final density from the entry profile, demonstrating small density uncertainty.

The density of the atmosphere was derived from probe decelerations through Newton's second law and the defining equation for drag coefficient,

$$D = (1/2)(\rho V^2)C_D A = ma \quad (1)$$

Here, D is the aerodynamic drag on the probe; ρ , the atmosphere density; V , the probe velocity; C_D , its drag coefficient; A , the frontal area, m , the probe mass; and a , the deceleration. Probe velocity was determined as a function of time by integrating the measured probe decelerations. Altitudes above the start of descent were determined by integrating the vertical component of

A. Seiff, Department of Meteorology, San Jose State University Foundation and MS 245-1, Ames Research Center, Moffett Field, CA 94035, USA.

D. B. Kirk, University of Oregon, 37465 Riverside Drive, Pleasant Hill, Oregon 97455, USA.

T. C. D. Knight, 2370 S. Brentwood St., Lakewood, CO 80227, USA.

L. A. Young, Center for Space Physics, Boston University, 725 Commonwealth Ave., Boston, Massachusetts 02215, USA.

F. S. Milos, M.S. 234-1, Ames Research Center, NASA, Moffett Field, CA 94035, USA.

E. Venkatapathy, Elore Institute, MS 230-2, Ames Research Center, Moffett Field, CA 94035, USA.

J. D. Mihalov and R. E. Young, MS 245-3, Ames Research Center, Moffett Field, CA 94035, USA.

R. C. Blanchard, MS 408A, Langley Research Center, NASA, Hampton, VA 23681, USA.

G. Schubert, Department of Earth and Space Sciences, University of California, Los Angeles, CA 90024, USA.

*To whom correspondence should be addressed. E-mail: aseiff@mail.arc.nasa.gov